

Adaptive Identification and Application of Flow Mapping for Electrohydraulic Valves

Jianbin Liu, André Sitte, Prof. Dr. -ing. Jürgen Weber*

Institute of Mechatronic Engineering - Chair of Fluid-Mechatronic Systems, Technical University of Dresden, Germany
E-mail: jianbin.liu@tu-dresden.de, andre.sitte@tu-dresden.de, fluidtronik@mailbox.tu-dresden.de

Abstract

Good estimates of flow mapping for electrohydraulic valves are important in automation of fluid power system. The purpose of this paper is to propose adaptive identification methods based on a recursive least squares method (RLSM), a recursive maximum likelihood method (RMLM) and radial basis function neural network (RBFNN) to estimate the uncertain parameters in flow mapping for electrohydraulic valves. In order to reduce the complexity and improve the identification performance, model structures derived from prior knowledge are introduced. The methods are applied to map the pressure-flow characteristic of an electrohydraulic valve. With the help of simulation results, the accuracy and efficiency of these algorithms are demonstrated. Some issues like invertibility of flow mapping are discussed and suggestions to apply these methods are made.

Keywords: adaptive identification, flow mapping, electrohydraulic valve, RLS, RML, RBF

1 Introduction

For many years, hydraulic-mechanical control systems have been characterized by extremely high requirements for good operability, high reliability, robustness and a favorable cost-benefit ratio. However, an increase in efficiency and productivity for control systems can only be achieved through the use of electrohydraulic components in combination with electronics, sensors and software. Among the many components that contributed to the success of electrohydraulic control systems, the proportional valve elements are of considerable importance. The flow rate of valves cannot be described precisely enough by simple physics-based equations because of highly non-linear characteristic. Offline-Identification of flow mapping is an efficient way to compensate the complex non-linearity in valves partially. Though offline-Identification cannot adapt to changes in the system properties over time, e.g. the influences of temperature, erosion on the valve edges and wear of valve spool. Therefore, a self-learning system for adaptive identification of flow mapping for proportional valve elements in electrohydraulic system is crucial, in which not only the complex non-linearity can be compensated, but also the flow mapping can be adapted to the varying system parameters. Numerous system identification methods are now available, but the suitability of adaptive identification for valve elements has not been sufficiently investigated. In addition, it is necessary to make a prediction based on limited data about flow mapping at some cases. As for the application of flow mapping, various fields can be found such as demand-based flow rate control for energy-efficient operation, high precision control, autonomous control, maintenance and fault detection, condition monitoring and diagnostics. The present paper aims to analyze different adaptive methods for (inverse) flow mapping which could be acted as feedforward controller. If the flow rate characteristic relationship $Q = f(U, \Delta p, \dots)$ is inverted to $U = f(Q, \Delta p, \dots)$, the inverse flow mapping could also be used for feedforward control instead of traditional lookup table method. Compared with the direct mapping for $U = f(Q, \Delta p, \dots)$, the inverse flow mapping can effectively reduce the complexity of computational effort while ensuring accuracy.

Starting with research and comparison of different adaptive identification methods, suitable for an adaptive identification of flow mapping in electrohydraulic valves, considering online-processing capability, signal-to-noise ratio, model fidelity and amongst others. Different adaptive identification method based on RLSM, RMLM and

RBFNN are chosen for flow mapping of electrohydraulic valves. Examples of adaptive identification with RLSM can be found in the work by Vahidi et al. [1], C. Kamali et al. [2], S. Dong et al. [3] and M. Kazemi et al. [4]. Similarly, RMLM is also the popular adaptive parameter estimation in the field of parameter identification. The origin of the RMLM can be traced back to R. A. Fisher [5]. L. Ma et al. [6] have applied the RMLM for the identification of Hammerstein ARMAX system and compared with RLSM in detail. In order to combine the advantages of Maximum Likelihood and RLSM, J. Li et al. [7] have used a maximum likelihood recursive least squares method for multivariable systems. Chen et al. [8] derived a filtering based maximum likelihood recursive least squares algorithm for reducing computational efforts. O. Nelles et al. [9] presented a comparison between RBF networks and classical methods for identification of nonlinear dynamic systems. RBFNN has wide applications in many areas such as computer science, aircraft and mathematics [10-14].

Besides the identification methods, the source data types play an important role in identification. Figure 1 proposes different source data types for identification. Static data are time independent. On the contrary, dynamic data are time dependent and the inertial effects have to be taken into account. The transition data type between them are quasi-static data, which are time dependent but slow enough to neglect its inertial effects. Usually, structured data characterize the flow behavior of throttle valves. These data are determined at discrete input signals, representing the operating range. There is a high resolution along the x-axis, whereas only a few data point exist along the y-axis. The data-gap increases the requirements for the training procedures (optimization) and eventually creates great deviations between model and estimation. A comprehensive scatter data-set appears to be advantageous in terms of coverage. However, arbitrary data is difficult to interpret and to evaluate, which is why the use of such data is not very widespread. Limited and noisy flow data are more common. The restrictions mostly result from limited capacities of the test rig or system setup. Noise is inherent to measurement data, which requires filtering of data or smoothing capabilities of the approximation procedures. Operating point data contain operating point resulting from a typical working cycle of machine. In this paper, quasi-static data combined with structured data and scattered data are used for identification.

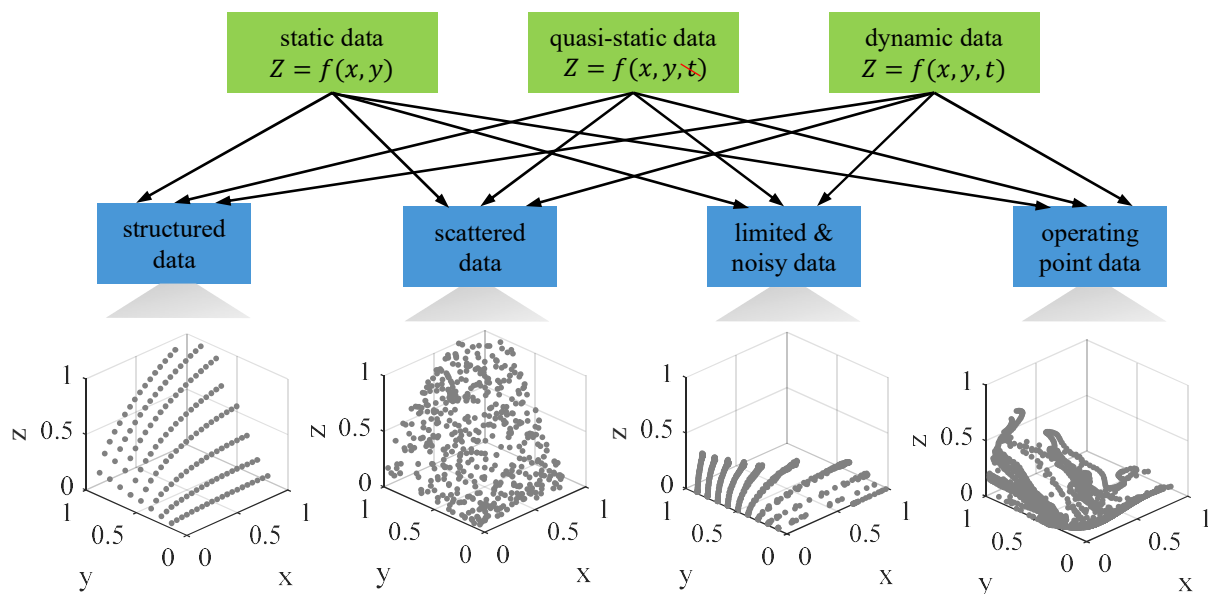


Figure 1: combination of source data types for identification [17]

The subsequent paper is organized as follows: In Section 2, to be acquainted with the static characteristics of the electrohydraulic valve, a test rig in laboratory has been set up. After that, a virtual demonstrator with real-time and streaming OPC UA data has been completed, which was carried out in simulation environment to validate the adaptive parameter identification methods. Then the suitable adaptive identification methods are chosen and derived in Section 3, including LSM, RLSM, RMLM and RBF. In Section 4, the previously developed, adaptive identification methods have been applied and exemplified in order to obtain the evolving flow mapping of a piloted proportional valve, which belongs to the test rig. The results demonstrate that the adaptive identification methods have convincing performance for the flow mapping of electrohydraulic valves. Finally, conclusions are drawn and some issues to be solved are discussed in Section 5.

2 Modelling and Test Rig of Electrohydraulic Valve

2.1 Modelling of Electrohydraulic valve

Figure 2 shows the construction of proportional seat valve “Valvistor”, which is based on hydraulic position feedback.

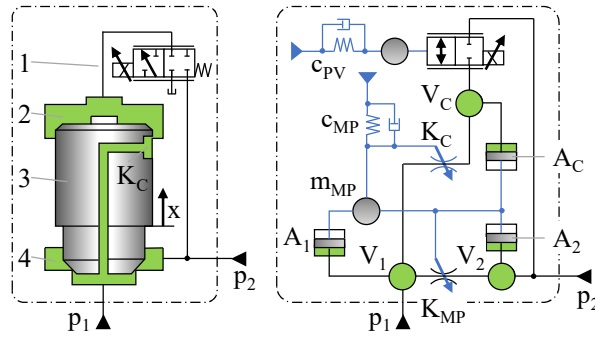


Figure 2: Construction for flow direction p_1 to p_2 (left)/ simplified simulation model structure (right) [17]

Due to a negative overlap of the variable orifice between control chamber (2) and main poppet (3), the pressure p_c in the control chamber V_c is equal to the pressure p_1 at the valve inlet V_1 . Because of the upper area of the main poppet is greater than the area facing p_1 , the closing position of seat valve is ensured. Opening the pilot valve (1), pressure drop enables the pilot flow Q_{PV} and reduces the control pressure p_c in the control chamber. The main poppet starts moving until the equilibrium of forces is established. Neglecting flow- and friction forces and rearranging the force balance equation for the main poppet leads to:

$$p_c = \frac{p_1}{\varphi} + \left(\frac{\varphi-1}{\varphi}\right) p_2 \text{ with } \varphi = \frac{A_1+A_2}{A_1} \quad (1)$$

The flow rate across control-orifice K_c results in:

$$Q_c = Q_{PV} = K_c(x_0 + x_{MP})\sqrt{\Delta p_{1c}} \quad (2)$$

Where x_{MP} is the displacement of main poppet and x_0 is the negative overlap. According to eq. (1) and (2), the following interrelation can be obtained:

$$x_{MP} = \left(\frac{Q_{PV}}{K_c} \sqrt{\frac{(\varphi-1)}{\varphi(p_1-p_2)}}\right) - x_0 \quad (3)$$

The flow rate across main poppet is given as:

$$Q_{MP} = K_{MP}x_{MP}\sqrt{\Delta p_{12}} \quad (4)$$

Neglecting the negative overlap x_0 in eq. (3) and substituting eq. (3) into eq. (4), results in following equation:

$$Q_{MP} = \left(\frac{K_{MP}}{K_c} \sqrt{\frac{\varphi-1}{\varphi}}\right) Q_{PV} \quad (5)$$

The total flow rate is given as:

$$Q_T = Q_{MP} + Q_{PV} \quad (6)$$

From eq. (5) and (6), it can be seen that Valvistor amplifies a small flow rate Q_{PV} through the pilot valve, which is similar to a transistor. Therefore, the name “Valvistor” is derived from valve and transistor. More about the Valvistor can be found in [15], [16] and [17].

2.2 Test Rig and Results

Figure 3 shows the hydraulic plan and corresponding test rig built in laboratory. It consists of hydraulic reservoir, adjustable pump, pressure relief valve, test valve (Valvistor), pressure control valve (load valve) and cooling system, which is not shown here. The instrumentations installed in the system are various pressure sensors, temperature sensor, a flow meter and displacement sensor, to measure the displacement of main poppet. For the static measurements, the hydraulic system could be seen as constant pressure system with $p_0 = 200$ bar. Because of limited power of pump, max. flow rate is restricted to $Q_{max} = 200$ l/min. Furthermore, in order to reduce

influence factor, the oil temperature in tank is set to $\vartheta_T = 40^\circ\text{C}$. To acquire the static characteristics of the electrohydraulic valve, the control signals for test valve are given in the manner of discrete values. At the same time, with the help of load valve, the outlet pressure p_2 varies between maximum and minimum so that the flow rate through test valve is changed in a quasi-static manner.

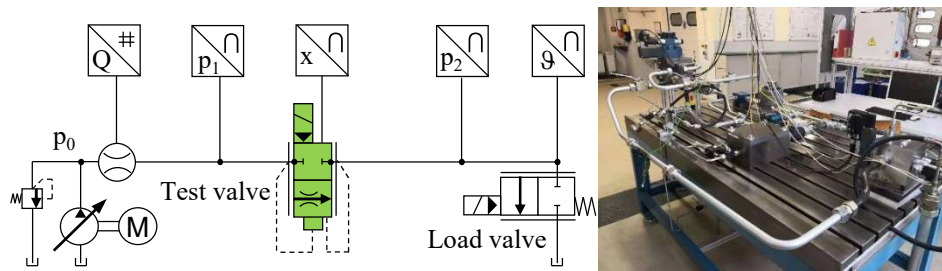


Figure 3: hydraulic plan for test rig (left) [17] Test rig in laboratory (right)

Figure 4 presents the flow rate-pressure drop characteristic curves of test valve at different control voltages. As a whole, the simulation results are in good agreement with the measured results. Based on the validated model, it's convenient to apply the adaptive identification methods in next section.

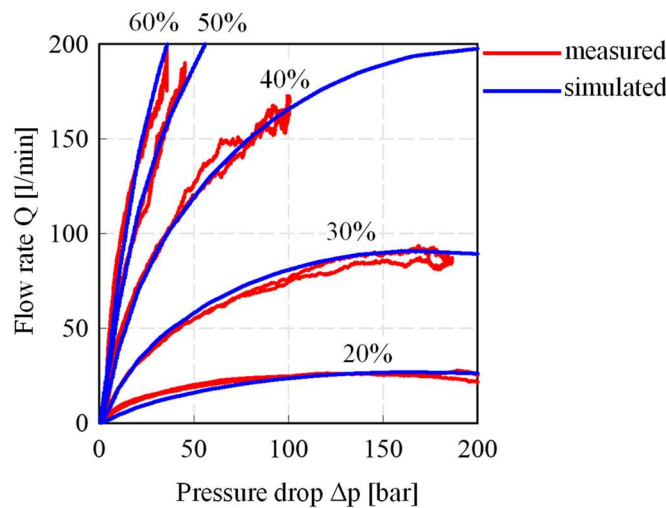


Figure 4: flow rate- pressure drop characteristic curves at different control voltages U_{rel}

3 Adaptive Identification Algorithm

3.1 Outline of Adaptive Identification

Figure 5 shows the simplified basic sequence of the identification. The first step is to define the purpose of identification. The purpose of this paper is to identify the relationship among flow rate Q , control voltage U and pressure drop Δp for electrohydraulic valves. With the help of a priori knowledge, it can be presented as:

$$Q = f(U, \Delta p)$$

The next step is determination of model structure. Model structure identification is based on the purpose of identification and the application of mathematical models in practice. Most of the mathematical model structures of linear systems can be easily identified by input and output data. However, since the static characteristics of electrohydraulic valves are more complex, which contain nonlinear factors, the model structures would mainly get through prior knowledge, assumptions and experiments. Based on these, there are two ways to determine the model structure.

The first way is to linearize the nonlinear system at first. Then use the linear system identification methods. This method will be adopted with RLSM and RMLM in the following. After trial tests, with the help of prior knowledge and algebraic polynomials [17], following approximation for the Valvisor valve can be given:

$$Q = f(U, \sqrt{\Delta p}) = a_1 + a_2 U + a_3 \sqrt{\Delta p} + a_4 U \sqrt{\Delta p} + a_5 (\sqrt{\Delta p})^2 \quad (7)$$

Where a_1, a_2, \dots, a_5 are the parameters, which should be identified. Pressure drop Δp is replaced by $\sqrt{\Delta p}$ in eq. (1). The reasons for that are closer to the theoretical flow rate formula and a kind of simple and efficient order-reduction means. By means of this linearization, it can greatly expand the scope of identification methods.

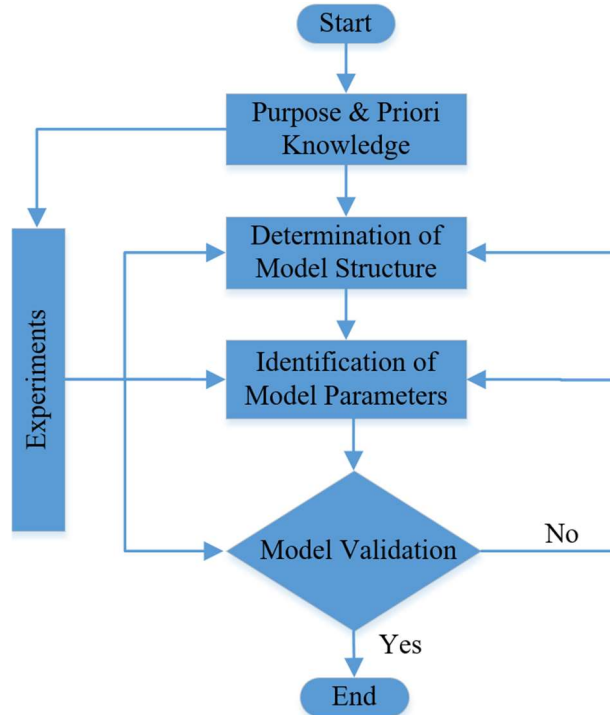


Figure 5: basic sequence of the identification [18]

Then the system approximation can be simplified as:

$$Q = X^T \theta \quad (8)$$

With $\theta = [a_1 \ a_2 \ a_3 \ a_4 \ a_5]^T$ and $X = [X_1 \ X_2 \ X_3 \ X_4 \ X_5]^T = [1 \ U \ \sqrt{\Delta p} \ U\sqrt{\Delta p} \ (\sqrt{\Delta p})^2]^T$.

The second method is to directly identify the nonlinear system model structure. For certain types of nonlinear system, models can be formulated that match well with the requirements on the model structure of known identification methods [18]. A nonlinear system identification using RBFNN will be covered in the following.

The following task is applying of suitable identification methods to identify model parameters. By means of a weighted point evaluation on the basis of the criteria suitability for linear or nonlinear process, allowable signal-to-noise ratio, suitability for offline or online processing, ability for time variant system and resulting model fidelity, preferred adaptive identification methods could be determined. At the end, least squares method (RLSM), recursive maximum likelihood method (RMLM) and radial basis function neural network (RBFNN) are therefore used for flow mapping of electrohydraulic valves and further investigated. Non-recursive least squares method (LSM) is introduced simply for derivation and comparison purposes in paper.

3.2 Non-Recursive Least Squares Method (LSM)

The non-recursive least squares method (LSM) can be utilized for linear systems. In general, the model estimation of electrohydraulic Valves is given as:

$$Q_M = a_1 X_1 + a_2 X_2 + \dots + a_n X_n \quad (9)$$

The error ε between measured output Q_P and model estimation Q_M is determined as:

$$Q_P = Q_M + \varepsilon = a_1 X_1 + a_2 X_2 + \dots + a_n X_n + \varepsilon \quad (10)$$

At different time $t = 1, 2, \dots, t$, it is easy to get the measured inputs X_i and output Q_P , which can be noted as $X_i(t)$ and $Q_P(t)$. Similarly, the error ε can be defined as $\varepsilon(t)$. Then the system equations can be written as:

$$\begin{cases} Q_p(1) = a_1X_1(1) + a_2X_2(1) + \dots + a_nX_n(1) + \varepsilon(1) \\ Q_p(2) = a_1X_1(2) + a_2X_2(2) + \dots + a_nX_n(2) + \varepsilon(2) \\ \vdots \\ Q_p(t) = a_1X_1(t) + a_2X_2(t) + \dots + a_nX_n(t) + \varepsilon(t) \end{cases} \quad (11)$$

If the vector θ and $X(t)$ are defined as $\theta = [a_1 \ a_2 \ \dots \ a_n]^T$ and $X(t) = [X_1(t) \ X_2(t) \ \dots \ X_n(t)]^T$. Then the system equation can be reduced to matrix form:

$$Q_p(t) = [X_1(t) \ X_2(t) \ \dots \ X_n(t)][a_1 \ a_2 \ \dots \ a_n]^T + \varepsilon(t) = X^T(t)\theta + \varepsilon(t) \quad (12)$$

If the vector $\mathbf{Q}_{p,t}$, \mathbf{X}_t and $\boldsymbol{\varepsilon}_t$ are defined as: $\mathbf{Q}_{p,t} = [Q_p(1) \ Q_p(2) \ \dots \ Q_p(t)]^T$, $\mathbf{X}_t = [X^T(1) \ X^T(2) \ \dots \ X^T(t)]^T$ and $\boldsymbol{\varepsilon}_t = [\varepsilon(1) \ \varepsilon(2) \ \dots \ \varepsilon(t)]^T$. Then the system equations (11) can be reduced to matrix form:

$$\mathbf{Q}_{p,t} = \mathbf{X}_t\theta + \boldsymbol{\varepsilon}_t \quad (13)$$

Where θ is the parameter vector, which should be identified. According the principle of least square, the cost function:

$$J(\theta) = \sum_{t=1}^L \varepsilon(t)^2 = \sum_{t=1}^L (Q_p(t) - X^T(t)\theta)^2 = \boldsymbol{\varepsilon}_t^T \boldsymbol{\varepsilon}_t = [\mathbf{Q}_{p,t} - \mathbf{X}_t\theta]^T [\mathbf{Q}_{p,t} - \mathbf{X}_t\theta] \quad (14)$$

To find the minimum of cost function, the first derivative with regard to the parameter vector θ is set to zero:

$$\left. \frac{\partial J(\theta)}{\partial \theta} \right|_{\hat{\theta}_{LS}} = -2\mathbf{X}_t^T(\mathbf{Q}_{p,t} - \mathbf{X}_t\theta) = 0 \quad (15)$$

This equation can be solved to provide an estimation for parameter vector $\hat{\theta}_{LS}$ as:

$$\hat{\theta}_{LS}(t) = (\mathbf{X}_t^T \mathbf{X}_t)^{-1} \mathbf{X}_t^T \mathbf{Q}_{p,t} = \left[\sum_{t=1}^L X(t)X^T(t) \right]^{-1} \left[\sum_{t=1}^L X(t)Q_p(t) \right] \quad (16)$$

Where L is the length of data.

3.3 Recursive Least Squares Method (RLSM)

The precondition for non-recursive least squares method (LSM) requires all the measured data had first been stored then estimates the parameter in one pass. Such a method requires also a lot of computational efforts, especially the matrix inversion in eq.(16). Therefore, the non-recursive least squares method (LSM) is not suitable for real time identification. In order to overcome these deficiencies, recursive least squares method (RLSM) is introduced. Furthermore, with appropriate modifications and forgetting factor, it's easy to realize the adaptive identification and solve the data saturation problem at the same time. With

$$P^{-1}(t) = \mathbf{X}_t^T \mathbf{X}_t = \sum_{t=1}^L X(t)X^T(t) = \sum_{t=1}^{L-1} X(t)X^T(t) + X(t)X^T(t)|_{t=L} \quad (17)$$

The following equation can be given:

$$P^{-1}(t) = P^{-1}(t-1) + X(t)X^T(t), \quad P(0) = P_0I > 0 \quad (18)$$

In order to reduce the error in matrix inversion of $P(t)$, according to matrix inversion lemma:

$$(A + BC)^{-1} = A^{-1} - A^{-1}B(I + CA^{-1}B)^{-1}CA^{-1}$$

The eq. (18) can be given as:

$$\begin{aligned} P(t) &= (P^{-1}(t-1) + X(t)X^T(t))^{-1} \\ &= P(t-1) - P(t-1)X(t)(1 + X^T(t)P(t-1)X(t))^{-1}X^T(t)P(t-1) \\ &= \left(I - \frac{P(t-1)X(t)X^T(t)}{1 + X^T(t)P(t-1)X(t)} \right) P(t-1) = (I - L(t)X^T(t))P(t-1) \end{aligned} \quad (19)$$

Where $L(t)$ is the gain vector:

$$L(t) = \frac{P(t-1)X(t)}{1 + X^T(t)P(t-1)X(t)} \quad (20)$$

Together with eq. (19) and (20), one then obtains:

$$P(t)X(t) = \left(I - \frac{P(t-1)X(t)X^T(t)}{1 + X^T(t)P(t-1)X(t)} \right) P(t-1)X(t) = \frac{P(t-1)X(t)}{1 + X^T(t)P(t-1)X(t)} = L(t) \quad (21)$$

According to the definition of $\mathbf{Q}_{P,t} = [Q_P(1) \ Q_P(2) \ \dots \ Q_P(t-1) \ Q_P(t)]^T = [\mathbf{Q}_{P,t-1} \ Q_P(t)]$ and $\mathbf{X}_t = [X^T(1) \ X^T(2) \ \dots \ X^T(t-1) \ X^T(t)]^T = [\mathbf{X}_{t-1} \ X^T(t)]$, the eq. (16) can be transformed as:

$$\begin{aligned} \hat{\theta}_{LS}(t) &= (\mathbf{X}_t^T \mathbf{X}_t)^{-1} \mathbf{X}_t^T \mathbf{Q}_{P,t} = P(t) \begin{bmatrix} \mathbf{X}_{t-1} \\ X^T(t) \end{bmatrix}^T \begin{bmatrix} \mathbf{Q}_{P,t-1} \\ Q_P(t) \end{bmatrix} = P(t) \left(\mathbf{X}_{t-1}^T \mathbf{Q}_{P,t-1} + X(t)Q_P(t) \right) \\ &= P(t) \left(P^{-1}(t-1)P(t-1)\mathbf{X}_{t-1}^T \mathbf{Q}_{P,t-1} + X(t)Q_P(t) \right) = P(t) \left(P^{-1}(t-1)\hat{\theta}_{LS}(t-1) + X(t)Q_P(t) \right) \end{aligned} \quad (22)$$

Base on eq. (18), one can substitute $P^{-1}(t-1) = P^{-1}(t) - X(t)X^T(t)$ in eq. (22) and obtains

$$\hat{\theta}_{LS}(t) = \hat{\theta}_{LS}(t-1) + P(t)X(t) \left(Q_P(t) - X^T(t)\hat{\theta}_{LS}(t-1) \right) \quad (23)$$

Which combined with eq. (21), one can write:

$$\hat{\theta}_{LS}(t) = \hat{\theta}_{LS}(t-1) + L(t) \left(Q_P(t) - X^T(t)\hat{\theta}_{LS}(t-1) \right) \quad (24)$$

From eq. (19), (20) and (24), recursive least squares method (RLSM) can be described by:

$$\begin{cases} L(t) = \frac{P(t-1)X(t)}{1 + X^T(t)P(t-1)X(t)} \\ \hat{\theta}_{LS}(t) = \hat{\theta}_{LS}(t-1) + L(t) \left(Q_P(t) - X^T(t)\hat{\theta}_{LS}(t-1) \right) \\ P(t) = (I - L(t)X^T(t))P(t-1) \end{cases} \quad (25)$$

If the estimation parameters of an electrohydraulic valve change abruptly, for example, damage of valve, RLSM can't capture the new values in time. The estimation parameter from RLSM will vary continuously but slowly, this is co called data saturation. With some modification, RLSM can be changed to RLSM with forgetting factor, in which less weight is given to older data and more weight to recent information. With new definition:

$$\mathbf{X}_t = \begin{bmatrix} \lambda^{\frac{1}{2}} \mathbf{X}_{t-1} \\ X^T(t) \end{bmatrix}$$

Where λ is the forgetting factor and $\in (0,1]$. The eq. (17) can be modified as:

$$P^\lambda(t) = \mathbf{X}_t^T \mathbf{X}_t = \sum_{t=1}^L X(t)X^T(t) = \frac{1}{\lambda} \sum_{t=1}^{L-1} X(t)X^T(t) + X(t)X^T(t)|_{t=L} = \frac{1}{\lambda} P^{-1}(t-1) + X(t)X^T(t) \quad (26)$$

Thus, it follows:

$$P^\lambda(t-1) = \frac{1}{\lambda} P^{-1}(t-1) \quad (27)$$

If one substitutes the eq. (27) in eq. (25), RLSM with forgetting factor is given as:

$$\begin{cases} L^\lambda(t) = \frac{P^\lambda(t-1)X(t)}{\lambda + X^T(t)P^\lambda(t-1)X(t)} \\ \hat{\theta}_{LS}(t) = \hat{\theta}_{LS}(t-1) + L^\lambda(t) \left(Q_P(t) - X^T(t)\hat{\theta}_{LS}(t-1) \right) \\ P(t) = \frac{1}{\lambda} \left(I - L^\lambda(t)X^T(t) \right) P^\lambda(t-1) \end{cases} \quad (28)$$

3.4 Recursive Maximum Likelihood Method (RMLM)

Unlike the deterministic parameters in RLSM, the parameter and output can be seen as random variables. In RMLM, the parameter vector θ has the probability density function $p(\theta)$ and the output vector $\mathbf{Q}_{P,t}$ is based on the conditional probability density function $p(\mathbf{Q}_{P,t}|\theta)$. According to the statistical property, RMLM can derive a solution to the parameter identification problem. Because of the space limitations, this paper can't give the derivation of recursive maximum likelihood method (RMLM). More Information about the derivation please to refer to [6] and [18]. RMLM for flow mapping is obtained as follows [6]:

$$\begin{cases} L(t) = P(t-1)h_f(t)(1+h_f^T(t)P(t-1)h_f(t))^{-1} \\ \hat{\varepsilon}(t) = z(t) - h^T(t)\hat{\theta}_{ML}(t-1) \\ \hat{\theta}_{ML}(t) = \hat{\theta}_{ML}(t-1) + L(t)\hat{\varepsilon}(t) \\ P(t) = (I - L(t)h_f^T(t))P(t-1) \end{cases} \quad (29)$$

With

$$\begin{cases} h(t) = [-z(t-1) \quad \dots \quad -z(t-n_a) \quad u(t-1) \quad \dots \quad u(t-n_b) \quad \hat{\varepsilon}(t-1) \quad \dots \quad \hat{\varepsilon}(t-n_d)]^T \\ h_f(t) = [-z_f(t-1) \quad \dots \quad -z_f(t-n_a) \quad u_f(t-1) \quad \dots \quad u_f(t-n_b) \quad \hat{\varepsilon}_f(t-1) \quad \dots \quad \hat{\varepsilon}_f(t-n_d)]^T \\ z_f(t) = z(t) - \hat{d}_1 z_f(t-1) \dots - \hat{d}_{n_d} z_f(t-n_d) \\ u_f(t) = u(t) - \hat{d}_1 u_f(t-1) \dots - \hat{d}_{n_d} u_f(t-n_d) \\ \hat{\varepsilon}_f(t) = \hat{\varepsilon}(t) - \hat{d}_1 \hat{\varepsilon}_f(t-1) \dots - \hat{d}_{n_d} \hat{\varepsilon}_f(t-n_d) \end{cases}$$

3.5 Radial Basis Function Neural Network (RBFNN)

RBFNN has recently drawn much attention due to their good generalization ability and a simple network structure that avoids unnecessary and lengthy calculation as compared to the multilayer feed-forward neural network (MFNN). RBFNN has three layers: the input layer X_i , the hidden layer H_j and the output layer Q_M , which are shown in Figure 6.

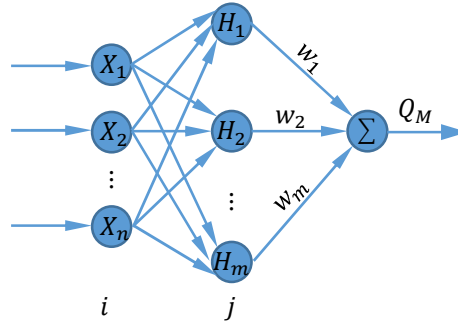


Figure 6: typical RBFNN structure

The input vector \mathbf{X} and radial basis function vector \mathbf{H} in RBFNN are defined as: $\mathbf{X} = [X_1 \quad X_2 \quad \dots \quad X_n]^T$ and $\mathbf{H} = [H_1 \quad H_2 \quad \dots \quad H_m]^T$ with $i = 1, 2, \dots, n$ and $j = 1, 2, \dots, m$. Where H_j is the Gaussian function value, which is given as:

$$H_j = \exp\left(-\frac{\|\mathbf{X} - C_j\|^2}{2b_j^2}\right) \quad (30)$$

Where $C_j = [c_{j1} \quad c_{j2} \quad \dots \quad c_{jn}]^T$ is the center vector of neural net j and b_j is the width of Gaussian function for neural net j . The width vector of Gaussian function can be given as $B = [b_1 \quad b_2 \quad \dots \quad b_m]^T$ & $b_j > 0$. Furthermore, the weight vector is $w = [w_1 \quad w_2 \quad \dots \quad w_m]^T$.

The output of RBFNN is:

$$Q_M(t) = Hw^T = H_1w_1 + H_2w_2 + \dots + H_mw_m \quad (31)$$

The cost function of RBFNN can be defined as:

$$\varepsilon(t) = \frac{1}{2}(Q_p(t) - Q_M(t)) \quad (32)$$

According to gradient descent method, RBFNN is given as:

$$\Delta w_j(t) = -\eta \frac{\partial \varepsilon(t)}{\partial w_j} = \eta(Q_p(t) - Q_M(t))H_j \quad (33)$$

$$w_j(t) = w_j(t-1) + \Delta w_j(t) + \alpha(w_j(t-1) - w_j(t-2)) \quad (34)$$

$$\Delta b_j(t) = -\eta \frac{\partial \varepsilon(t)}{\partial b_j} = \eta(Q_p(t) - Q_M(t))w_j H_j \frac{\|X - C_j\|^2}{b_j^3} \quad (35)$$

$$b_j(t) = b_j(t-1) + \Delta b_j(t) + \alpha(b_j(t-1) - b_j(t-2)) \quad (36)$$

$$\Delta c_{ji}(t) = (Q_p(t) - Q_M(t))w_j \frac{x - c_{ji}}{b_j^2} \quad (37)$$

$$c_{ji}(t) = c_{ji}(t-1) + \eta \Delta c_{ji}(t) + \alpha(c_{ji}(t-1) - c_{ji}(t-2)) \quad (38)$$

Where $\eta \in (0, 1)$ is the learning rate and $\alpha \in (0, 1)$ is momentum factor.

4 Results Analysis and Verification

The last step is the performance evaluation of the identified methods, the so-called verification by comparison of measured plant output Q_p and predicted model output Q_M . In order to identify the parameters of the electrohydraulic valve, following structured data in Figure 7 are used. To get the system excited enough, the signals cover the total operating range $U \in [0, 100]\%$ and $\Delta p \in [0, 200]$ bar.

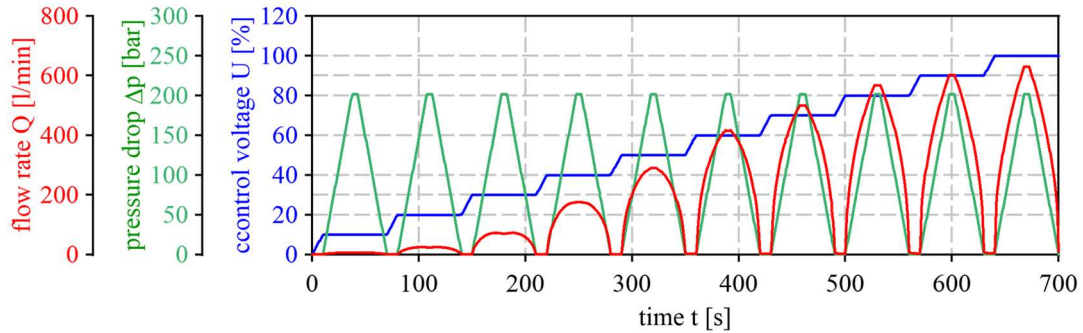


Figure 7: process of structured data to identify

In order to identify the parameters of the electrohydraulic valve, following scattered data in Figure 8 can be also utilized. For a better comparison, the signals cover the same range $U \in [0, 100]\%$ and $\Delta p \in [0, 200]$ bar like in structured data.

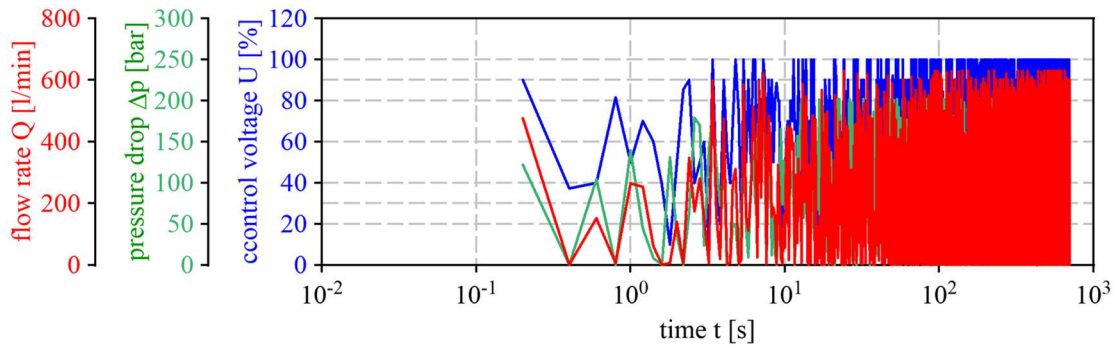


Figure 8: process of scattered data to identify

In order to illustrate the merit of the above-mentioned methods, it is appropriate to use the following signals for verification purposes. The test data include data that does not exist in the training data.

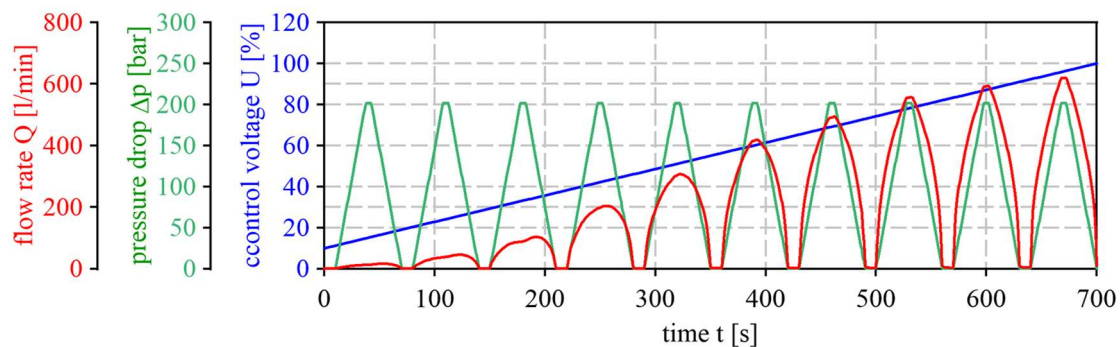


Figure 9: process of input and output data to verify

Table 1 shows verification of RLSM using different forgetting factors and RBFNN with structured data. In order to compare the goodness of identification for the different methods, the estimated flow rate Q_M are plotted against the real flow rate Q_P from test data. With an ideal identification, all points would lie exactly on the 45° red diagonal curve. For RLSM with different forgetting factors, the well-known phenomenon of parameters “fluctuation” can be deduced during increase of forgetting factor. It is noted that decreasing the forgetting factor will only worsen the situation. It could be found that RLSM with $\lambda = 0.995$ cannot get convergence at the end. If the forgetting factor is set to 1 ($\lambda = 1$), RLSM with forgetting factor will be degenerated as classical LSM, which will eliminate the fluctuation. However, classical LSM deals with all the past data equally and can result in data saturation problem. Therefore, it is necessary to select suitable forgetting factors in practice. Under the premise of predicted accuracy guarantee, the parameters fluctuation should be controlled at reasonable area at the same time. Compared with RLSM, the merit of RBFNN is the best fitting results regarding accuracy at the end, although the rate of convergence is slow. From these comparisons in Table 1, the conclusion can be drawn that RLSM with forgetting factor shows better extrapolating behavior than RBFNN. Both methods show suitable identification results. Furthermore, to use the identified flow mapping of valve, the characteristic interrelation $Q = f(U, \Delta p)$ needs to be inverted to $U = f(Q, \Delta p)$. In terms of invertibility, it's obvious that RLSM with model structure in eq.(7) is easy to transform. Whereas, it is very hard to get explicit mathematical description directly from RBFNN. A feasible way is to reidentify and change the inputs, output and model structure at the same time. As for RMLM, this method with structured data cannot converge to desired results. Therefore, it doesn't show up in the table. About the reasons for non-convergence, please refer to problems of convergence of maximum likelihood iterative procedures in multi-parameter situations by N. Mantel et al. [19].

Table 2 shows verification of RLSM under different forgetting factors and RMLM with scattered data. For RLSM with different forgetting factors, problems of convergence can also be seen during increase of forgetting factor. Compared with structured data, a wider range of forgetting factors is tolerable with scattered data. Without consideration for difficulty in data acquisition, methods with scattered data are much faster than methods with structured data in terms of the rate of convergence. Compared to RLSM, RMLM shows almost the same results regarding accuracy at the end, although the rate of convergence is slower. Regarding of RMLM, previous non-convergence problem in structured data seems to have been solved with scattered data. In conclusion, both of methods show good identification results. As for RBFNN, this method with scattered data cannot converge to desired results. Therefore, it doesn't show up in the Table 2. In RBFNN, the parameters of c_{ji} and b_j must be adjusted according to the scope of the input values. For arbitrary scattered data, the parameters are adjusted inappropriately, Gaussian function will not be effectively mapped and RBF network will be invalid [20]. Summarizing, the gradient descent method is not suitable to adjust c_{ji} and b_j in RBFNN with scattered data.

By contrast, RLSM with forgetting factor is more suitable for real application. At first, RLSM with forgetting factor is able to deal with all kinds of data types. Furthermore, another advantage of RLSM with forgetting factor in contrast to other methods is that it enables to integrate multi-dimensional dependencies with a reduced set of parameters in the software development for embedded systems. Unlike RLSM, an implementation of RBFNN in embedded systems could be problematic, since massive floating-point calculations are inevitable. Regarding to the fitting quality of RLSM, one way to improve the accuracy is to adopt partition identification for local area. The second way is to increase order in eq. (7) until the accuracy meets the requirements.

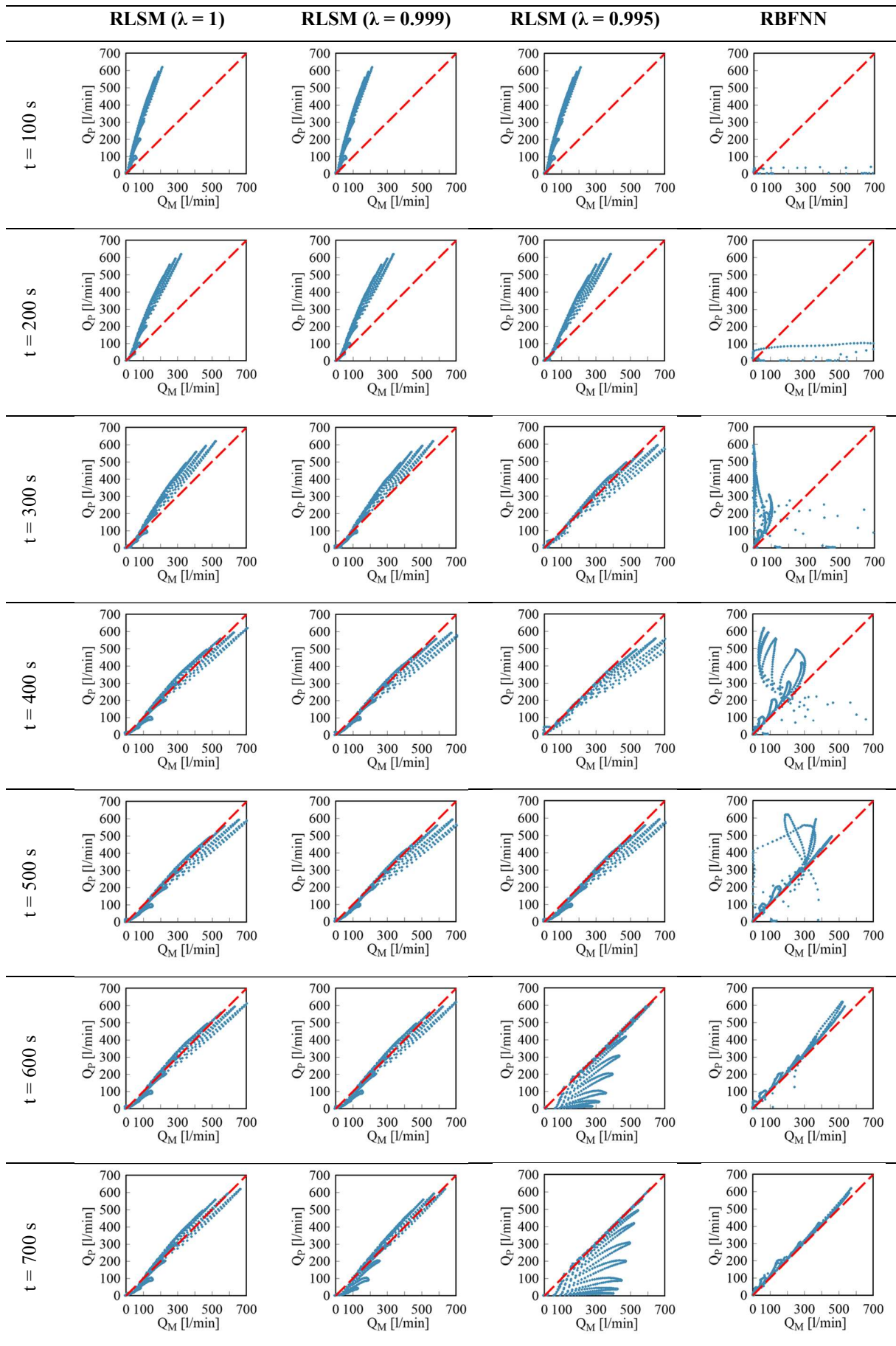


Table 1: Verification of RLSM and RBFNN with structured data

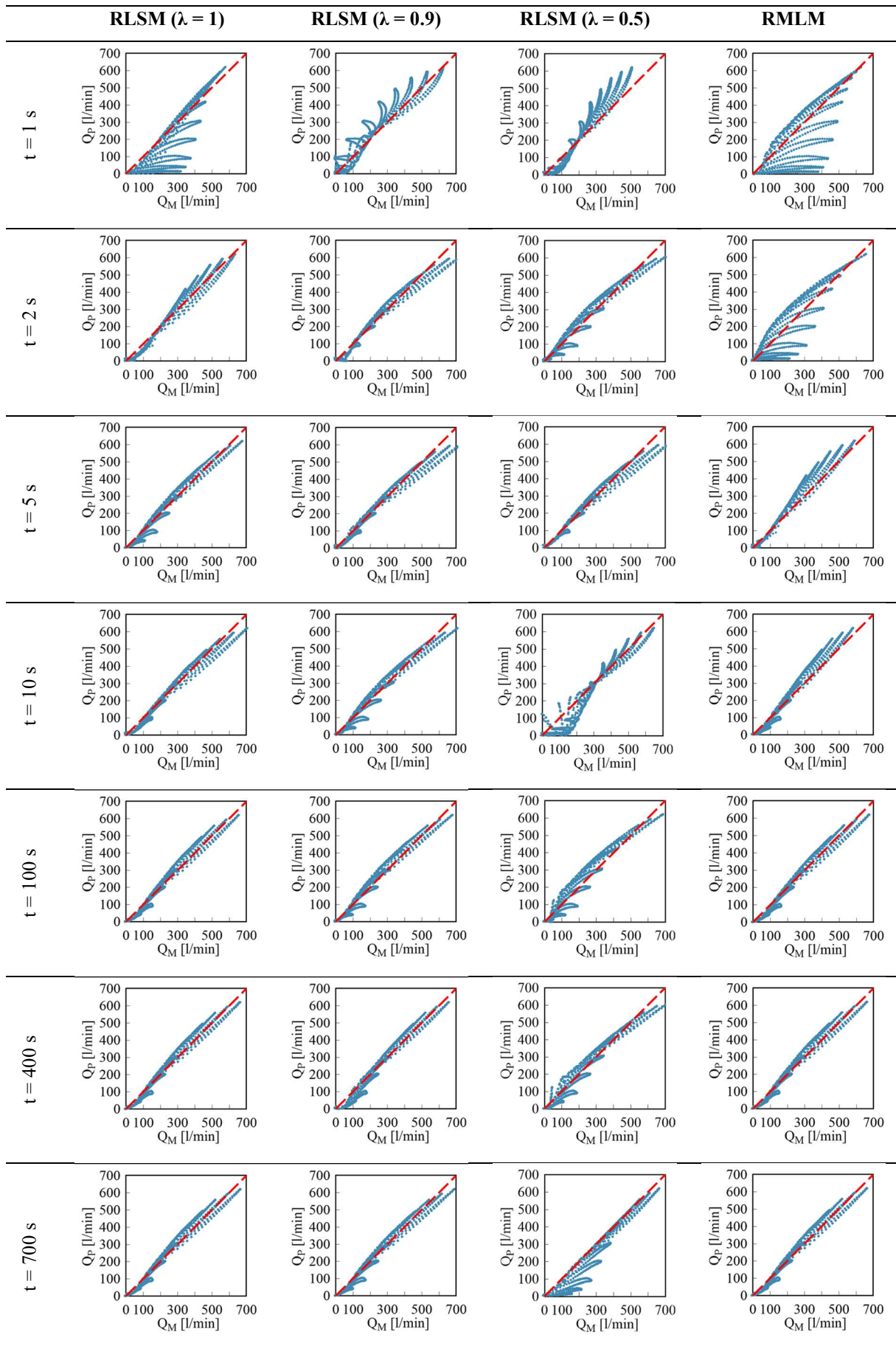


Table 2: Verification of RLSM and RMLM with scattered data

5 Conclusion and Outlook

In this research, the different flow mapping identification methods for electrohydraulic valves are proposed. This paper presented an analysis and comparison of different identification methods and data structures for 3D-flow mapping. The proposed methods can be applied to adaptive identification for real machines in the future and occupies small memory capacity at the same time. Moreover, their identification accuracy and convergence property have been sufficiently investigated.

So far, the flow mapping identification methods have been applied for only one valve with little hysteresis and at a constant temperature. In order to improve the generalization of the methods and obtain a flow mapping with higher precision, the next investigation steps are concerned with the further development of the proposed methods with respect to 4D-flow mapping or even more such as temperature and hysteresis. After that, the inverse multidimensional flow mapping in precision motion control applications should be further tested. At last, it is worth mentioning that some research on dynamic characteristics of the electrohydraulic valve with help of same test rig has been done. Identification for dynamic characteristics of electrohydraulic valves as the next challenging task would be further studied.

Nomenclature

Designation	Denotation	Unit
F_i	Force	N
a_1, a_2, \dots, a_n	Estimated parameters	-
A	Matrix	-
A_1	Piston area of main poppet in inlet	mm ²
A_2	Ring area of main poppet in outlet	mm ²
b_j	Width vector	-
B	Matrix	-
c_{ji}	Parameter in center vector	-
C	Matrix	-
C_j	Center vector	-
d_i	Coefficient for error vector	-
\hat{d}_i	Estimated Parameter in Parameter vector for noise	-
$h(t)$	Data vector	-
$h_f(t)$	Revised data vector	-
\mathbf{H}	Radial basis function vector	-
H_1, H_2, \dots, H_m	Gaussian function value	-
I	Index	-
I	Unit Matrix	-
L	Gain vector	-
j	Index	-
$J(\theta)$	Cost function	-
K_C	Flow coefficient of control-orifice	l/min·bar ^{-0.5} ·mm ⁻¹
K_{MP}	Flow coefficient of main poppet	l/min·bar ^{-0.5} ·mm ⁻¹
p_0	Constant system pressure	bar
p_1	Pressure in valve inlet	bar
p_2	Pressure in valve outlet	bar
p_c	Pressure in the control chamber	bar
$P(t)$	Data matrix	-
P_0	Initial data matrix	-
Q	Flow rate through valve	l/min
Q_C	Flow rate through control-orifice	l/min
Q_{max}	Max. Flow rate through main poppet	l/min
Q_M	Estimated flow rate for valve(model)	l/min
Q_{MP}	Flow rate through main poppet	l/min
Q_P	Measured flow rate for valve(plant)	l/min
$\mathbf{Q}_{P,t}$	Measured flow rate vector	-
Q_{PV}	Flow rate through pilot valve	l/min

Q_T	Total flow rate through valve	l/min
t	Time	s
$u(t)$	Input data	-
$u_f(t)$	Revised input data	-
U	Input voltage for valve	V
V_1	Valve chamber in inlet	mm ³
V_2	Valve chamber in outlet	mm ³
V_C	Control chamber in valve	mm ³
w_1, w_2, \dots, w_m	Weight vector	-
x	Input variable	-
x_{MP}	Displacement of main poppet	mm
x_0	Negative overlap of control-orifice	mm
X	Matrix for inputs	-
\mathbf{X}	Input vector	-
X_1, X_2, \dots, X_n	Input parameters in input matrix	-
\mathbf{X}_t	Input parameters matrix	-
y	Input variable	-
$z(t)$	Output data	-
$z_f(t)$	Revised output data	-
Z	Output variable	-
Δp	Pressure drop through valve	bar
Δp_{12}	Pressure drop between inlet and outlet	bar
Δp_{1C}	Pressure drop between inlet and control chamber	bar
α	Momentum factor	-
ε	Error	-
$\hat{\varepsilon}_f$	Estimated Error	-
ε_t	Error matrix	-
φ	Area ratio	-
ϑ	Temperature	°C
ϑ_T	Temperature in tank	°C
θ	Vector for estimated parameter	-
$\hat{\theta}_{LS}(t)$	Estimated parameter vector in LSM	-
$\hat{\theta}_{ML}(t)$	Estimated parameter vector in MLM	-
λ	Forgetting factor	-
η	Learning rate	-
<i>ARMAX</i>	Autoregressive moving average with exogenous	
<i>MFNN</i>	Multilayer feed-forward neural network	
<i>OPC UA</i>	Open Platform Communications Unified	
<i>RLSM</i>	Recursive least squares method	
<i>RMLM</i>	Recursive maximum likelihood method	
<i>RBNN</i>	Radial basis function neural network	

References

- [1] A Vahidi, A Stefanopoulou and H Peng. *Recursive least squares with forgetting for online estimation of vehicle mass and road grade: theory and experiments*. Mechanical Engineering Dept., University of Michigan, Ann Arbor
- [2] C Kamali, A A Pashikar and J R Raol. *Evaluation of recursive least squares algorithm for parameter estimation in aircraft real time applications*. *Aerospace Science and Technology* 15, P. 165-174, 2011.
- [3] S Dong, L Yu, W A Zhang and B Chen. *Robust extended recursive least squares identification algorithm for Hammerstein systems with dynamic disturbances*. *Digital Signal Processing* 101, 102716, 2020
- [4] M Kazemi and M M Arefi. *A fast iterative recursive least squares algorithm for Wiener model identification of highly nonlinear systems*. *ISA Transaction*, 2016

- [5] R A Fisher. *On the mathematical foundations of theoretical statistics*. Fellow of Gonville and Caius College, Cambridge, P. 309-368, 1922
- [6] L Ma and X Liu. *Recursive maximum likelihood method for the identification of Hammerstein ARMAX system*. Applied Mathematical Modelling 000, P. 1-13, 2016
- [7] J Li, F Ding, P Jiang and D Zhu. *Maximum Likelihood Recursive Least Squares Estimation for Multivariable Systems*. Circuits, Systems and Signal Processing 33, P. 2971-2986, 2014
- [8] F Chen and F Ding. *The filtering based maximum likelihood recursive least squares estimation for multiple-input single-output systems*. Applied Mathematical Modelling 000, P. 1-13, 2015
- [9] O Nelles and R Isermann. *A Comparison Between RBF Networks and Classical Methods for Identification of Nonlinear Dynamic Systems*. IFAC Adaptive Systems in Control and Signal Processing, P 233-238, 1995
- [10] M Y Mashor, *Some properties of RBF network with applications to system identification*. IJCIM Volume 7, P. 1-37 1999
- [11] H Yijun and N Wu. *Application of RBF Network in System Identification for Flight Control Systems*. 2010 International Forum on Information Technology and Applications (IFITA), P. 67-69, 2010
- [12] C Pislaru and A Shebani. *Identification of Nonlinear Systems Using Radial Basis Function Neural Network*. International Scholarly and Scientific Research & Innovation, Vol. 8, P. 1528-1533, 2014
- [13] J B d A Rego, A d M Martins and E d B Costa. *Deterministic System Identification Using RBF Networks*. Mathematical Problems in Engineering, Vol. 2014, P. 1-10, 2014
- [14] S Khan, I Naseem, R Togneri and M Bennamoun. *A Novel Adaptive Kernel for the RBF Neural Networks*. Circuits Systems and Signal Processing. Band 36. P. 1639-1653, 2017
- [15] B R Andersson. *On the Valvistor, a proportionally controlled seat valve*. Linköping Studies in Science and Technology. Dissertations. No. 108, 1984
- [16] E Prasetyawan, R Zhang, und A Alleyne. *Fundamental performance limitations for a class of electronic two-stage proportional flow valves*. Proceedings of American Control Conference, P. 3955-3960, 2001
- [17] A Sitte, O Koch, J Liu, R Tautenhahn, J Weber. *Multidimensional flow mapping for proportional valves*. 12th International Fluid Power Conference, Dresden, Group F, P. 231-240, 2020
- [18] R Isermann, M Münchhof. *Identification of Dynamic Systems – An Introduction with Applications*. ISBN 978-3-540-78878-2, P. 324-332, 2011
- [19] N Mantel, M Myers. *Problems of convergence of maximum likelihood iterative procedures in multiparameter situations*, Journal of the American Statistical Association, Vol.66, No.335, P. 484-491, 1971
- [20] J Liu, *Radial Basis Function (RBF) Neural Network Control for Mechanical Systems*, Springer Berlin Heidelberg, P. 24, 2013